JAAS

Accepted Manuscript

This is an *Accepted Manuscript*, which has been through the Royal Society of Chemistry peer review process and has been accepted for publication.

Accepted Manuscripts are published online shortly after acceptance, before technical editing, formatting and proof reading. Using this free service, authors can make their results available to the community, in citable form, before we publish the edited article. We will replace this *Accepted Manuscript* with the edited and formatted *Advance Article* as soon as it is available.

You can find more information about *Accepted Manuscripts* in the Information for Authors.

Please note that technical editing may introduce minor changes to the text and/or graphics, which may alter content. The journal's standard Terms & Conditions and the Ethical guidelines still apply. In no event shall the Royal Society of Chemistry be held responsible for any errors or omissions in this *Accepted Manuscript* or any consequences arising from the use of any information it contains.

ROYAL SOCIETY OF CHEMISTRY

www.rsc.org/jaas

DETERMINATION OF PLASMA IGNITION THRESHOLD FLUENCE DURING FEMTOSECOND SINGLE-SHOT LASER ABLATION ON METALLIC SAMPLES DETECTED BY OPTICAL EMISSION SPECTROSCOPY

Marina López-Claros, José M. Vadillo and J. Javier Laserna*

Universidad de Málaga, Departamento de Química Analítica 29071 Málaga, España

ABSTRACT

The minimum laser fluence needed for plasma ignition on a sample during single-shot femtosecond laser ablation has been determined for a set of metals and alloys. Threshold fluence values ranged between 4 and 9 J cm^{-2} for ablation craters with a diameter of 40 μm. Craters exhibited similar size and shape regardless the sample type, energy range (for energies per pulse < 400 μJ) and accumulated energy dosage (< 500 laser shots on the same sample position). The results obtained for the metals (Pb, Ag, Zn, Sn, Cr, Cu, W, Ni and Fe) show a clear trend of the fluence threshold with the work function, evidencing the importance of the surface electron excitation in femtosecond laser-matter interaction. Experiments with the alloyed samples reveal that fluence thresholds for femtosecond plasma ignition are matrix independent.

KEYWORDS: Ultrafast ablation, Femtosecond, Microanalysis, LIBS, Matrix effects.

INTRODUCTION

The laser fluence (energy per surface area) used to irradiate a sample is one of the parameter that determines the type of thermal process leading to material loss from its surface, typically vaporization, normal boiling or explosive boiling. The prevailing process depends on the laser pulse duration as well as on the temperature attained in the irradiated material. Several analysis techniques take advantage of the ablation process to perform qualitative or quantitative characterization of solid samples. Among them, optical emission spectroscopy of the expanding plasma formed during explosive boiling (LIBS, laser-induced breakdown spectroscopy) represents one of the most versatile, widely accepted surface analysis technique[1] capable of facing complex problems both in lab and in the field. One of the most complex scenarios where LIBS can be compete with other techniques is in the single-event microanalysis, where all the required information must be obtained from a one and only laser shot. Under such boundary condition, it is strictly required to set the experimental parameters to values where signal is detected at reproducible fashion with minimum sample damage.

The laser ablation threshold fluence (F_{th}) is the minimum laser energy per surface unit required to initiate the removal of constituents from a target surface. As long as the knowledge of the starting of sample damage is important for many applications related to surface alteration, microprocessing or eye surgery to name a few, F_{th} represents a key parameter to be determined. In LIBS, additional fluence over the F_{th} is required to reach the phase explosion associated to the explosive boiling conditions and initiate plasma emission (the so-called plasma formation threshold fluence, ${}^{Pl}F_{th}$). While F_{th} must be determined by observation of the surface damage, ${}^{Pl}F_{th}$ can be measured by different methods including electrical probes, or different types of spectroscopies. In LIBS, the appearance of the laser plasmas over the sample surface is determined by optical emission spectroscopy[2], although in applications conducted under vacuum conditions, mass spectrometry[3] or simultaneous ion/photon detection schemes[4,5] may be followed.

Under nanosecond excitation, the dominant thermal ablation mechanism prevailing during plasma formation induces a large heat-affected zone (HAZ) in the sample what generates ablation craters much larger than the laser spot diameter. High quality LIBS spectra are obtained, but at the expense of sample damage, loss of lateral resolution or element alloying. Even under threshold conditions, subsurface alteration in the sample has been observed by focused ion beam sections of the affected sample area.[6] Obviously, the extent of the HAZ depends on the excitation conditions. Different experimental strategies based on the combined use of short wavelengths, excellent laser spatial profiles and very short focal lengths allow the generation of craters with diameters in the low micrometric range. Particularly promising is the combination of nanosecond LIBS with near-field focusing systems[7] that has been tried with success from the point of view of the minimum eroded material. Unfortunately, the low emission yield (detected signal per unit of ablated mass) and the sample requirements to make it operative (particularly the sample flatness) make such approach difficult to implement in a regular basics.

Early micromachining applications of femtosecond lasers[8] showed craters free from thermal effects, triggering the interest for their use in LIBS as an alternative to nanosecond lasers[9]. The explanation of such behavior relies on the so-called two temperature model[10] that governs its physics. Once the femtosecond laser pulse hits the sample surface, free electrons in the target material absorb the photon energy through a multiphoton process, rising up its temperature. Electron thermalization occurs through heat transfer to the lattice by a process controlled by the electron to lattice relaxation timethat occurs in a timescale of a few picoseconds. This temporal separation between electron and bulk excitation has been observed by time-resolved images[11] that have also evidenced both the generation of a early surface electron plasma in the very first picoseconds, and the expansion of the vapor plume several hundred picoseconds after the laser pulse. Depending on the thermo-physical properties of the target material, the timescale of this process takes from a fraction of a picosecond to tens of picoseconds. Since the lattice does not heat appreciably during the pulse, there is no modification of electron-lattice scattering rates and no need

to track the flow of energy into the lattice to account for thermal and mechanical stresses, as is necessary with pulses of longer duration[12]. The energy of the incoming pulse conditions the energy transfer from the electron subsystem to the atomic lattice that may experience dislocation, surface alteration, ablation or plasma formation.[13]

Femtosecond LIBS represents an excellent alternative to keep all the advantages in terms of sampling flexibility and speed that have turned LIBS into a widely used technique, without the drawbacks derived from its inherent thermal nature.[14] Although for bulk analysis heat effects may not represent a big issue, the reduction of HAZ for microanalysis allows the achievement of better lateral resolutions. In combination with a near-field optical set-up, ${}^{Pl}F_{th}$ was calculated in 5 J cm^{-2} in a 200 nm Cr thin film deposited on a quartz wafer over craters with a diameter of 650 nm.[15] The criterion used for the assignment of the threshold was based on the appearance of discrete Cr peaks with a specific signal-to-noise ratio on the recorded spectrum acquired by single-shot laser excitation. Despite the excellent results, the applicability to the analysis of complex samples with elements present in minor concentration seems to be challenging yet due to the low sensitivity of the technique.

The present work examines femtosecond LIBS with the aim of determining working conditions suitable for microanalysis of multicomponent samples close to the threshold fluence. Some works have mentioned in the past that reduction in laser fluence may affect the stoichiometry of the ejected material (and that of plasma) due to the selective ablation (elemental fractionation) of elements with less melting point.[16] Based on the previous experience with nanosecond excitation and mass spectrometry of binary and ternary alloys,[3] the ionization threshold of different elements in a given sample was different than that of the individual elements as pure samples. Thus, the threshold value in the samples was related with the average thermal properties of the individual constituents: the presence in the matrix of elements of high melting point turn the whole sample more refractory. Emission thresholds of different metals as pure or alloyed form in plasmas induced with 35 fs laser pulses are reported. Under the minimization of thermal effects in the femtosecond

laser ablation it is not expected a dependence of the threshold values with thermal properties of the sample. The determination of the fluence emission threshold for each element in pure form will be related to different chemical and physical properties and compared to that in an alloyed sample. Based on the physics of the laser-matter interaction under femtosecond pulses, the role of early surface electrons can be significant. As in previous papers,[3,4] the criterion followed for threshold determination consists on precise measurements of micrographies of the craters. The laser energy was controlled by optical attenuation of the beam, and a criterion for the threshold determination based on individual spectrum rather than in accumulative ones was followed looking for the suitable scenery for single-shot microanalysis with LIBS.

EXPERIMENTAL

Figure 1 represents schematically the fs-LIBS setup. The laser consists on a Ti:sapphire oscillator providing a laser beam centered at 800 nm with a pulse energy of 400 nJ and a pulse duration of 400 fs. Due to the large bandwidth of the beam (aprox. 60 nm) it is amplified under the principle of chirped pulse amplification.[17] After amplification, a 35-fs pulse width laser output centered at 800 nm, with a maximum energy per pulse of 3.5 mJ is obtained. The pulse duration of the fs-pulses was measured with an autocorrelator. The stabilities of energy and pulse width were measured after every measurement run to keep variability below 1%. The fine control of the pulse energy was performed by rotation of a λ/4 crystal in combination with a polarizer at Brewster angle. To guarantee the reproducibility of the results, the crystal angle was modified to obtain specific energy values over the desired range at 10 μJ steps. The laser was delivered by a set of mirrors and focused onto the sample surface using a plane-convex quartz lens with 250 mm focal length. The beam diameter was 10 mm before focusing. The sample was fixed directly with conductive tape in a sample-holder attached to a rotary motor to allow the permanent irradiation of fresh surface. Optical emission of the plasma plume was collected at 90º with a 330-mm focal length lens and 1:1 imaged onto the entrance slit of a 0.5 m focal-length Czerny-Turner grating spectrograph equipped with an intensified charge-coupled device as a detector. Light was dispersed using the 1200 grooves mm^{-1} grating. The entrance slit was 10 μm wide and 10 mm high.

Samples were foils of Ag, Sn, Pb, Zn, Cu, Ni, Fe, Cr and W with a nominal thickness between 250 μm and 1000 μm and purity better than 99.9% (Sigma-Aldrich), binary alloys (Fe/Ni, Fe/Cr, and Ni/Cr from MBH), ternary alloy (Fe/Cr/Ni from MBH) and a stainless steel of known composition (ACERINOX, Spain). The alloyed samples were cut in 1-mm thick squared pieces of 10 x 10 mm to fit in the sample holder. The samples were rinsed with water, methanol and acetone and were left dry in air before the analysis. The composition of the alloys is summarized in Table 1. In order to obtain information about the sample, the following signals were monitored: Ag (I) at

520.90 nm; Sn(I) at 326.23 nm; Pb(I) at 405.78 nm; Zn(I) at 481.0 nm; Cu(I) at 521.82 nm; Ni (I) at 352.45 nm; Fe(I) at 440.47 nm; Cr(I) at 425.43 nm and W(I) at 400.87 nm.

RESULTS AND DISCUSSION

Several aspects were taken into account before starting the experiments due to the peculiarities of the pulse-compression technology for femtosecond lasers. A key aspect to account with is the complex temporal structure of energy distribution of a femtosecond laser, that potentially includes amplified spontaneous emission, residual pulse train from the femtosecond oscillator, and pre- or post- pulses due to non-perfect extinction ratio of the internal Pockels driving the regenerative amplification in the laser. Each of these structural components of the temporal energy distribution could induce pre-excitation of the surface which may have a strong effect on the material thresholds.[18] Careful reduction of the pre- and post-pulses were done by fine tuning of the extraction delay of the regenerative amplifier before starting the experiments with the help of a fast photodiode coupled to a digital oscilloscope, and checking the autocorrelation trace.

Experimental determination of the plasma formation thresholds was performed by careful controlling the energy deposited on the sample and monitoring the individual events generated. This procedure is similar to that followed on previous references.[3,4] Spectroscopic parameters are optimized to obtain the maximum signal intensity using a delay time of 60 ns and a gate width of 100 ns. Such conditions were selected after time-resolved studies of the light emitted from the plasma, looking for maximum sensitivity. A flat, polished and cleaned sample was placed on a sample holder connected to a rotary motor that allowed the recording of individual LIBS spectrum at fresh surface positions. This procedure was followed in order to look for a realistic scenario where a single-shot operation mode is followed. Under such sampling conditions, signal averaging does not apply, and a well-defined criterion must be followed to fix the threshold condition. Our studies were initially performed in a pure Fe foil by modifying the energy reaching the sample. The energy threshold was calculated by recording sets of 20 individual spectra at fixed laser energy per pulse and a fixed pulse width of 35 fs. Different spectra sets correspond to increased energy values. The Fe(I) intensity signal at 440.47 nm was divided by the average background signal (around 635 counts) and plotted. Figure 2 shows the signal-to-background ratio (SBR) for the 20 individual

spectra covering a range from 60 to 130 μJ per pulse. At energies per pulse lower than 60 μJ, none of the 20 individual spectra was able to provide a measurable signal.

The observation of the individual pulses, evidence the need of establishing a criteria to select a threshold value. To differentiate the peak from the background, we consider that the SBR must be higher than 1.05. In our experiments, such value corresponds to a signal-to-noise ratio (SNR) of 10, the well-established criteria for the limit of quantification. On top of that, we forced an additional condition: the SBR> 1.05 criteria must be fulfilled for each individual data. Achieving this criterion, the energy threshold for the Fe sample was established at 100 μJ. Again, it is important to note that such strict conditions are based on the need of assuring the recording of spectra under the worst-case scenario where the only chance is a single shot on a specific location.

Once the criterion for the threshold energy was established, a second part of the work did consist on the determination of the area of the sample affected by the beam. A knife-edge procedure[2] represents the most accurate procedure to measure the beam area reaching the sample. However, based on the lack of thermal affection in the femtosecond ablation, the visual differences in the roughness of the laser-affected zone represents a good estimation as well. Figure 3 shows a crater formed after 20 shots of 35 fs at an energy of 100 μJ. The incoming beam exhibited a Gaussian profile, visible in the sample as the laser affected zone (LAZ). Considering that 86% of the energy of the beam is confined in a radius defined by $1/e^2$ from the center, it is expected that the central part of the LAZ represents the minimum laser affected zone (MLAZ). In the zoomed region in Figure 3, the different regions corresponding to the energy gradients are visible. The inner region (zone c), corresponds to the center of the spot in which the material is fully melted. The tails of the incoming pulse (representing a 14% of its energy) are responsible of the second circle or alteration (zone b). Depending on the pulse energy, this zone may have energy large enough to produce detectable photons. Finally, an outer region (zone a) is present with characteristics ripples well studied for laser-induced patterning surface structuring.[19]

Increasing the energy of the incoming beam does not modify significantly the craters in the energy range where the plasma formation threshold occurs. Figure 4 shows the effect of 20 laser shots of 35 fs on a polished Fe foil at increasing pulse energies from 60 μJ to 100 μJ. As observed, regardless the energy, the MLAZ has a measured diameter of 40 μm (1.25×10^{-3} mm^2) with absent heat-diffusion effects spreading the affected area. More significantly, the MLAZ remained identical for the set of samples and alloys used in the energy per pulse regime used in this work. It is important to mention that the MLAZ value measured agrees with the theoretical value for the limit of diffraction for a Gaussian beam under the experimental conditions used. Importantly, the MLAZ value did not increased for laser energies up to 400 μJ, and kept constant even for 500 accumulated shots, evidencing the absence of deleterious heat-related effects. Obviously, the increased depth was evident under the cited circumstances, far from optimum for single-shot microanalysis.

The same procedure described in Figure 2 for Fe was followed for other metals: Pb, Ag, Zn, Sn, Cr, Cu, W and Ni. For each material the process to determine the plasma ignition fluence was followed, covering an energy range between 40 μJ and 130 μJ per pulse (a fluence range between 3.2 J cm^{-2} and 10.3 J cm^{-2} for a spot diameter of 40 μm) at 10 μJ steps. Values between 4 J cm^{-2} and 9 J cm^{-2} were obtained for the different metals, and were plotted against different thermal and optical properties. In principle, only the work function did exhibit an acceptable correlation (0.8) with ${}^{Pl}F_{th.}$ It is clear that a perfect adjustment based on a single parameter for such a complex process can´t be expected. However, the correlation observed in Figure 5 for the work function indicates a significant relevance of such parameter. It is important to mention that the work function values used in Figure 5[20] are based on average values for polycrystalline samples. Several effects such as micro roughness, oxidation state or sample impurities modify slightly the tabulated values and so, could improve the linearity of the results. Considering the laser-matter interaction during femtosecond ablation, the work function dependence observed is understandable as the promotion of initial electrons from the valence band to the vacuum level is required for the building up of the high intense electric field that will lead to Coulomb expansion and plasma formation.[21]

Once determined the emission fluence values for the different pure elements, the study was focused on checking the dependence of the values obtained with the matrix. In a previous work with nanosecond excitation and ion detection[3] it was found that matrix played a significant role, introducing variations as large as 25% in the calculated values of the emission threshold of a given element as pure sample with respect to its emission threshold in alloyed form. The effect of the femtosecond irradiation was checked on the same set of samples. Table I shows the sample composition in Cr, Ni and Fe. Any other element is present at concentrations below 0.5%. The results are graphically depicted in Figure 6. The plot shows the fluence value for the three elements as pure foils as well as in the six alloyed samples. The experiment shows very clearly that the fluence value for each element is not affected by the matrices used. In the case of Ni, for example, the concentration range in the alloyed samples covers from 10 to 80% and the threshold value remains at 8.7 J cm^{-2}. The same is noticed for Fe and Cr.

Differences in the elemental composition of an alloy modify significantly their thermal properties, and so affect the behavior of the ablation process during nanosecond excitation. The experiments performed have shown that in binary and ternary alloys the use of femtosecond laser ablation reduces the dependence of fluence threshold for plasma ignition from the thermal properties of the sample as a whole, to turn more dependent of the work function of the individual elements present. The generation of laser plasmas enriched in specific components from a complex matrix by tuning the fluence above or below that of the elements of interest is currently open and under study.

CONCLUSIONS

Femtosecond laser-induced breakdown spectroscopy (LIBS) adds to conventional nanosecond-based LIBS in the reduction of thermal effects during laser-matter interaction. Such property allows the reduction of the ablation craters close to their limits of diffraction, a beneficial situation for single-shot microanalysis applications. The paper has determined the threshold fluence value for plasma formation on different pure metallic samples and alloys. In order to guarantee the recording of signal under single-shot conditions, a strict criterion based on the limit of quantification (SNR = 10) was applied. The results obtained for the metallic samples (Pb, Ag, Zn, Sn, Cr, Cu, W, Ni and Fe) shows a clear trend of the fluence threshold with the work function, evidencing the importance of the surface electron excitation in the femtosecond laser-matter interaction. The experiments with the alloyed samples reveal that the fluence thresholds for femtosecond laser are matrix independent. For analysis in single-shot mode, the fact that all the elements, regardless the matrix, keep the same fluence threshold as in pure form is relevant. On the one side, it allows a previous optimization with pure samples to perform the analysis under specific conditions for a given element. On the other hand, a selected fluence value could be below the fluence threshold value for other elements present in the sample. This fact should be accounted in the applications implying depth-resolved analysis of materials with layers of element with significant differences in ${}^{Pl}F_{th}$. For single-shot analysis on multielemental samples it will be required the use of the energy of the element with the higher ${}^{Pl}F_{th}$. In this sense, this fact induces to think that certain elemental fractionation may occur in the plasma whose extension must be object of future works.

ACKNOWLEDGEMENTS

The work has been funded by the Spanish Minstry of Economy and Competitiveness through the proyect CTQ2011-24433. One of the authors (MLC) acknowledges the Andalusian Regional Goverment the research grant associated to the project.

FIGURE LEGENDS

Figure 1. Scheme (not to scale) of the experimental setup used. BS: Beam splitter; AC: Autocorrelator; Ph: Photodiode; VA: Variable attenuator; EM: Energy meter; ICCD: Intensified Charge Coupled Device.

Figure 2. Variation of the SBR for Fe as a function of the energy. Set of 20 individual spectra data at fixed laser energy per pulse was recorded covering a range from 60 to 130 μJ. The $^{Pl}E_{th}$ for Fe sample is taken as the energy value providing an SBR >1.05 for every independent shot in the data set.

Figure 3. Scanning-electron microscopy images of a crater produced on a polished Fe foil by the incoming femtosecond gaussian beam after 20 shots of 50 fs at an energy of 100 μJ. On the right, a section is zoomed out, showing three different zones corresponding to the energy gradients of the beam laser. See additional explanation in the text.

Figure 4. Scanning-electron microscopy images of craters produced on a polished Fe surface by 20 laser pulses of 50 fs with energies of (a) 60, (b) 80 and (c) 100 μJ with the same sample and focal position. The three craters have at the same MLAZ (40 μm in diameter) delimited by the white dashed line.

Figure 5. Correlation between work function with the measures for plasma formation threshold fluence calculated as described in the text.

Figure 6. Comparison of the $^{Pl}F_{th}$ values between pure elements (Fe, Ni and Cr) and six alloyed samples at different percentage of composition.

REFERENCES

1. J.M. Vadillo and J.J Laserna, *Spectrochim. Acta B*, 2004, **59**, 147.
2. L.M. Cabalín and J.J. Laserna, *Spectrochim. Acta B*, 1998, **53**, 723.
3. J.F. Alcántara, J.M. Vadillo and J.J Laserna, *J. Anal. At. Spectrom.*, 2010, **25**, 1424.
4. J.M. Vadillo, C.C. García, J.F. Alcántara and J.J Laserna, *Spectrochim. Acta B*, 2005, **60**, 948.
5. T. Delgado, J.M. Vadillo and J.J. Laserna, *J. Anal. At. Spectrom.*, 2013, **28**, 1377.
6. H. Téllez, J.M. Vadillo, R.J. Chater, J.J. Laserna and D.S. McPhail, *Appl. Surf. Sci.*, 2008, **255**, 2265.
7. D.J. Hwang, C.P. Grigoropoulos, J. Yoo and R.E. Russo, *Appl. Phys. Lett.*, 2006, **89**, 254101.
8. X. Liu, D. Du and G. Mourou, *IEEE J. Quantum Electron.*, 1997, **33**, 1706.
9. V. Margetic, A. Pakulev, A. Stockhaus, M. Bolshov, K. Niemax and R. Hergenröder, *Spectrochim. Acta B*, 2000, **55**, 1771.
10. J. Reif, *Basic physics of femtosecond laser ablation in Laser-surface interactions for new materials production*, Springer, 2010.
11. S.S. Mao, X. Mao, R. Greif, and R.E. Russo, *Appl. Phys. Lett.*, 2000, **77**, 2464.
12. B.C. Stuart, M.D. Feit, S. Herman, A.M. Rubenchik, B.W. Shore and M.D. Perry, *Phys. Rev. B*, 1996, **53**, 1749.
13. E.L. Gurevich and R. Hergenröder, *Appl.Spectrosc.*, 2007, **61**, 233A.
14. S. Musazzi, U. Perini, *in Laser-Induced Breakdown Spectroscopy*, Chapter 6, Springer, 2014.
15. D.J. Hwang, H. Jeon, C.P. Grigoropoulos, J.Y. Yoo, and R.E. Russo, *Appl. Phys. Lett.*, 2007, **91**, 251118.
16. C.C. Garcia, H. Lindner, A. Bohlen, C. Vadla and K. Niemax. *J. Anal. At. Spectrom*., 2008, **23**, 470.

17. D. Strickland and G. Mourou, *Opt. Commun.*, 1985, **56**, 219.

18. N. Sanner, O. Utéza, B. Bussiere, G. Coustillier, A. Leray, T. Itina and M. Sentis. *Appl. Phys. A*., 2009, **94**, 889.

19. E. Rebollar, J.R. Vázquez de Aldana, J.A. Pérez-Hernández, T.A. Ezquerra, P. Moreno and M. Castillejo. *Appl. Phys. Lett.*, 2012, **100**, 041106.

20. H. B. Michaelson, *J. Appl. Phys.*, 1977, **48**, 4729.

21. E.G. Gamaly, *Phys. Rep.*, 2011, **508**, 91.

Table 1 Chemical composition (% weight) of the alloys used in this work.

Alloy	Elemental Abundance (%)		
	Cr	Fe	Ni
Fe/Ni (MBH 13589J)	-	BAL	49.6
Fe/Ni (MBH 13763F)		BAL	10.1
Fe/Cr (MBH 13765G)	19.9	BAL	-
Ni/Cr (MBH Nimonic)	19.9	1.15	BAL
Fe//Ni/Cr (MBH Incoloy)	20.17	BAL	32.7
Stainless steel (AISI 304)	18	70	8

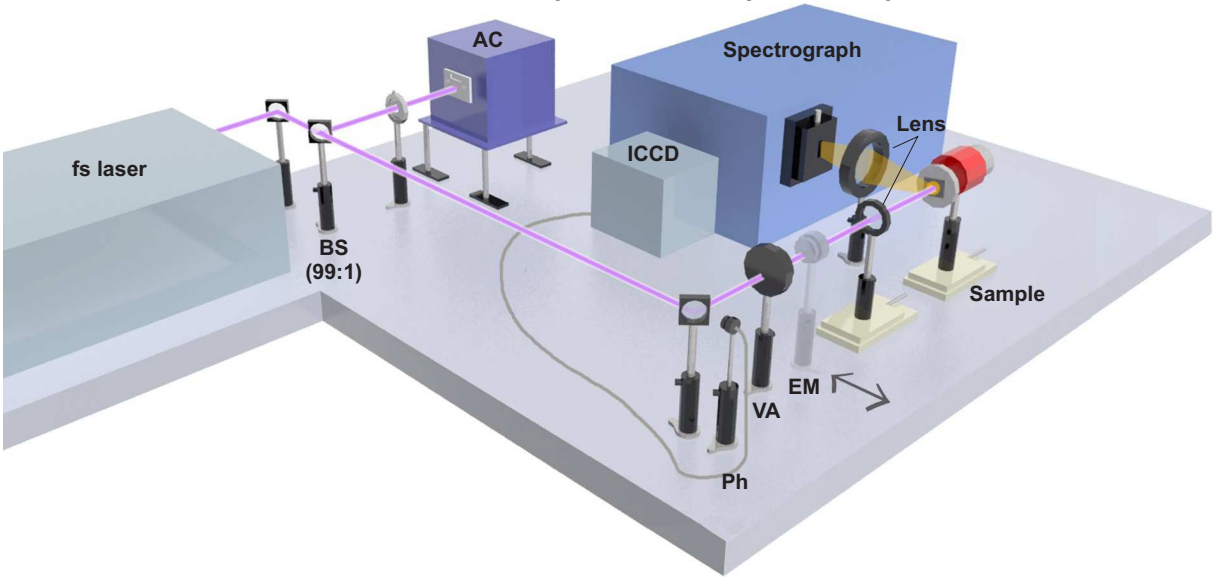

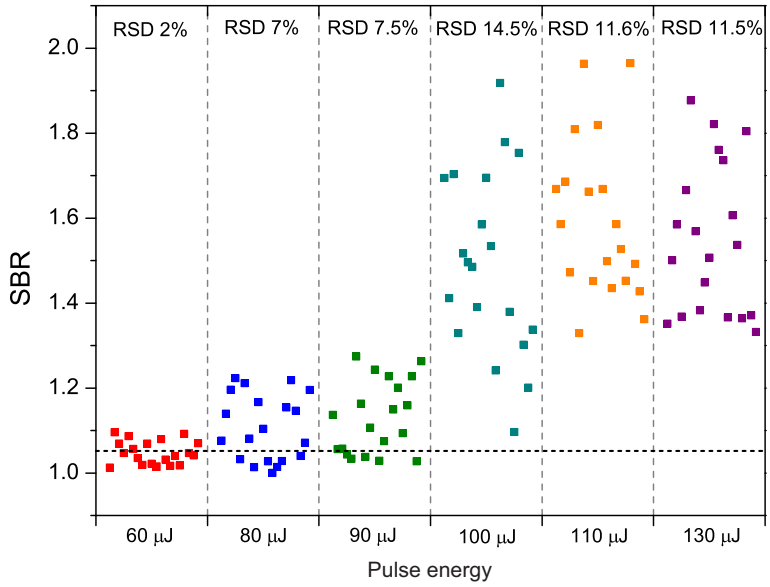

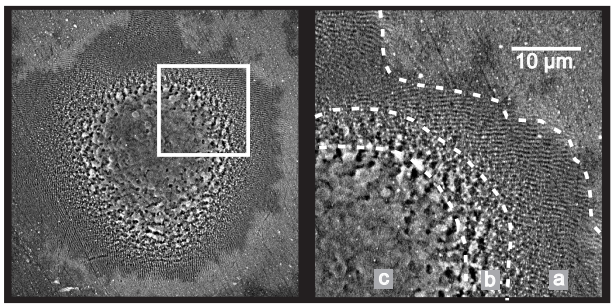

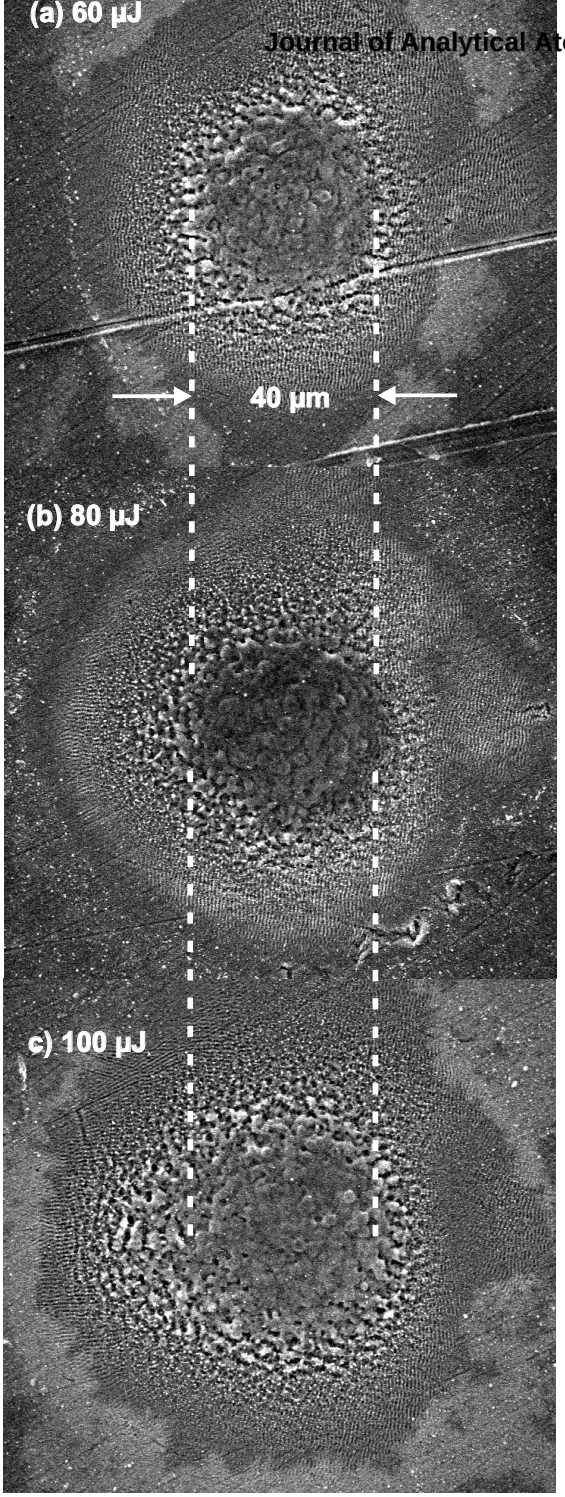

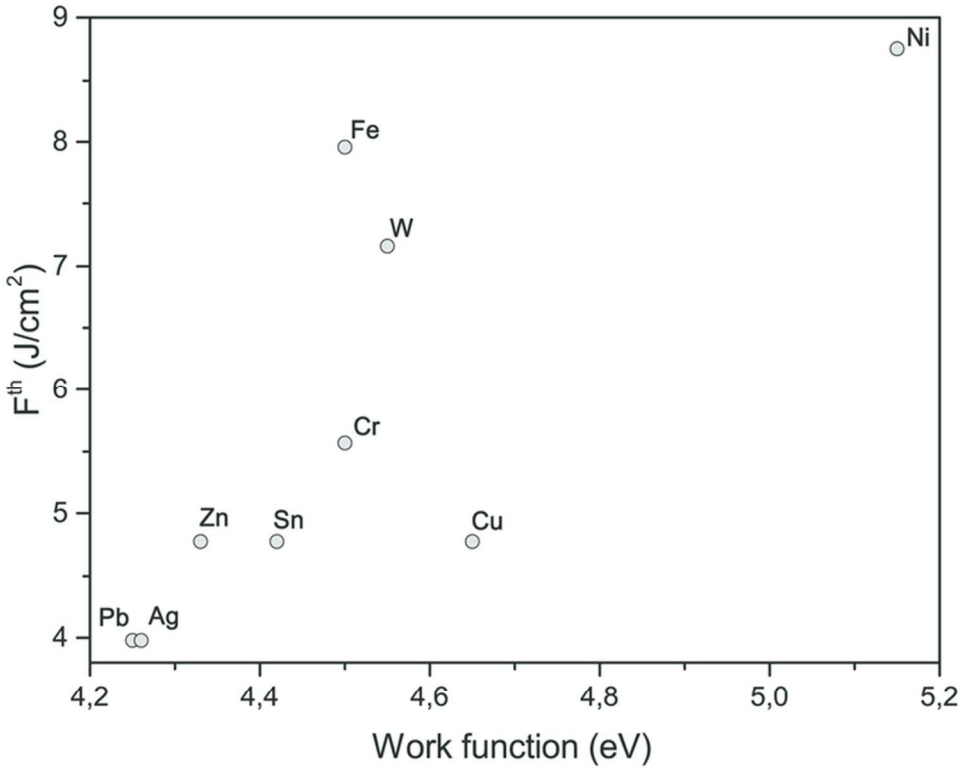

68x55mm (300 x 300 DPI)

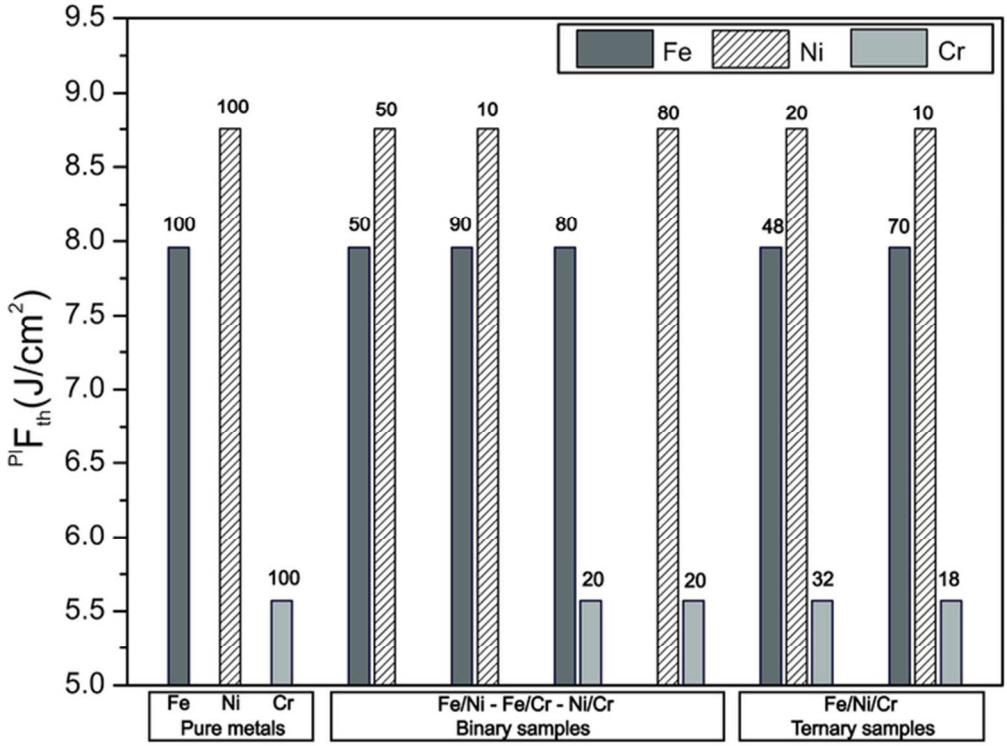

60x45mm (300 x 300 DPI)